

# Pose Adjustment Considering Linear Cross-Section Continuity of Line-Structured Light-Based 3D Tunnel Measurements

Takuya Igaue<sup>1</sup>, Toko Hayamizu<sup>1</sup>, Kenichi Yoshida<sup>2</sup>, Satoshi Yamanaka<sup>2</sup>, Hajime Asama<sup>1</sup> and Atsushi Yamashita<sup>3</sup>

**Abstract**—In this paper, we propose a method to reduce the position estimation error of line-structured light-based 3D measurements using two unmanned aerial vehicles (UAVs). In addition to the camera used for cross-section measurements, the proposed method uses a camera for pose estimation. The pose of the two cameras can be estimated by performing a 2D–3D registration using an additional camera. Therefore, by alternatively moving both cameras, it is possible to perform 3D measurements of long sections in tunnels. In this method, the measurement procedure is divided into multiple measurement cycles. This process results in two errors. First, as the UAV cannot halt completely in the environment, a drift in the cross-section positions occurs. Second, the rotation of the integrated point cloud of each cycle is inaccurate owing to the pose estimation inaccuracy of the cross-section. To solve the first error, we stabilized the ray vectors using landmarks in the environment. To solve the second error, we compensated for the point cloud rotation based on the fact that the cross-section moves in a straight line at the joints of each measurement area. In the experiments, we performed 3D measurements of a model tunnel with no curvature. The proposed method suppressed the cross-section point cloud drift. In addition, we could calculate the position of the tunnel cross-section with an error of 212 mm in the axial direction, where the error was the largest, over a distance of 30 m.

## I. INTRODUCTION

Three-dimensional (3D) measurements are commonly performed during tunnel construction to evaluate the geometry of the construction objects and improve safety. One of the applications of 3D point clouds is the detection of the surface of the tunnel lining and ground deformations. In particular, if the geology of the tunnel is not uniform, local ground deformations may occur in the tunnel [1]. In addition, there is the possibility of defects in appurtenances, such as support structures, at tunnel construction sites [2]. Therefore, dense tunnel 3D measurements are required during tunnel construction. When taking measurements at tunnel construction sites, the ground can often be muddy or under construction (e.g., invert work), and it is therefore advantageous to use an unmanned

aerial vehicle (UAV) to perform the 3D measurements as it does not travel on the ground.

LiDAR (light detection and ranging) [3] and terrestrial laser scanners [4]–[6] are commonly used for 3D tunnel measurements. These instruments are based on the time-of-flight method, which calculates the distance to a single location based on the propagation time of light. For large structures, the measured points from LiDARs tend to be sparse. Therefore, it is desirable to realize denser 3D measurements. Line-structured light-based methods [7] are used to achieve denser measurements. One of these methods uses an omnidirectional laser [8]–[10] that emits a 360° laser beam and can perform 3D measurement on a cross-section in a single shot. Therefore, it would be useful to detect local deformations in a tunnel using a dense 3D point cloud with 3D measurements based on this line-structured light method using an omnidirectional laser.

To obtain a 3D point cloud of the entire tunnel from the cross-section point clouds, the coordinate systems of the measured cross-sections must be integrated. One method for estimating the movement of a measurement device is measuring the change in camera pose using the color texture in the environment [11]. However, the lack of texture in tunnels causes a disastrous error during coordinate system integration.

Matching 3D geometry is a method for coordinate system integration that does not rely on environmental texture [12], [13]. However, for tunnels with monotonous geometry, it may not be possible to resolve the misalignment along the road direction. Meanwhile, the cooperative use of multiple devices enables the estimation of movement without using the environmental texture [14]. However, this requires a large measurement device because the LiDAR for 3D measurement and the total station for pose estimation must be attached to the device. Therefore, to carry the system, a large UAV is required, which may not be able to traverse the tunnels. Therefore, it would be advantageous to estimate the movement using fewer sensors.

Igaue et al. [15] performed pose estimation by adding a camera to a cross-section measurement device based on a line-structured light method. This method uses the cross-section shape of the structure pointed by the omnidirectional laser for cross-section pose estimation. Thus, it enables the integration of the coordinate system of the measured cross-section from only two cameras and an omnidirectional laser. Furthermore, the action cameras and laser can be mounted on a UAV. However, as shown in Fig. 1, this method has

<sup>1</sup>T. Igaue, T. Hayamizu and H. Asama are with the Department of Precision Engineering, Graduate School of Engineering, The University of Tokyo, 5-1-5 Kashiwanoha, Kashiwa, Chiba 277-8563, Japan {igaue, hayamizu, asama}@robot.t.u-tokyo.ac.jp

<sup>2</sup>K. Yoshida and S. Yamanaka are with the Department of Tunneling Technology Development, Obayashi Corporation, 2-15-2 Konan, Minato-ku, Tokyo 108-8502, Japan {yoshida.kenichi.ro, yamanaka.satoshi}@obayashi.co.jp

<sup>3</sup>A. Yamashita are with Department of Human and Engineered Environmental Studies, Graduate School of Frontier Sciences, The University of Tokyo, 5-1-5 Kashiwanoha, Kashiwa, Chiba 277-8563, Japan yamashita@robot.t.u-tokyo.ac.jp

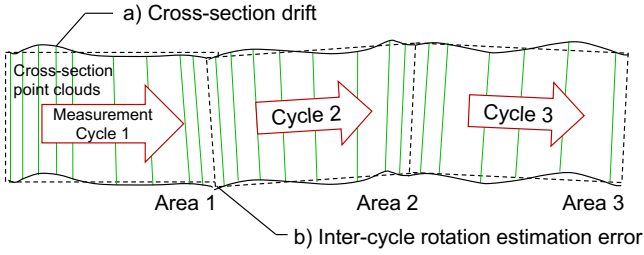


Fig. 1. Errors occurring in the measurement system with alternating UAVs.

two problems: a) When the system is mounted on the UAV, position estimation errors occur owing to the drift of the UAV. b) The cross-section pose estimation error causes rotation estimation errors between measurement cycles. If large errors occur in the pose estimation of the measured cross-section point cloud, it is difficult to obtain the accurate positions of the detected deformations or defects in the tunnel. Therefore, it is important to reduce these errors and measure 3D point clouds with higher accuracy.

The objective of this study is to reduce the errors in 3D tunnel measurement based on the line-structured light method using two UAVs. To achieve this, the position estimation errors caused by the drift of the UAVs were compensated. Furthermore, pose adjustment was performed between the measurement cycles to reduce the position estimation errors of the cross-sections.

The contributions of this paper are as follows:

- 1) The drift effects of the cross-section point clouds were reduced in the line-structured light-based 3D measurements using two UAVs. Environmental landmarks were used for ray vector stabilization of the camera.
- 2) The pose estimation error of the point cloud for each measurement cycle was reduced. Linearity in the direction of the cross-section was used for pose adjustment of the point clouds.

## II. PROPOSED METHOD

An overview of the proposed method is shown in Fig. 2. The first step in this method is performing a 3D measurement of a long section of a tunnel by alternately moving two measurement devices. For the relative position estimation of the two devices, 2D–3D registration is performed to integrate the coordinate systems of the measured cross-sections. As the second step, the drift error of the cross-sections is corrected by stabilizing the ray vector of the camera on the UAV using the landmarks in the tunnel. Finally, pose adjustment of the point cloud in each measurement cycle is performed to solve the rotation estimation error at the joints of the measurement cycles. The error reduction ensures highly accurate coordinate system integration of the measured point clouds, even when long areas of the tunnel are measured at a time.

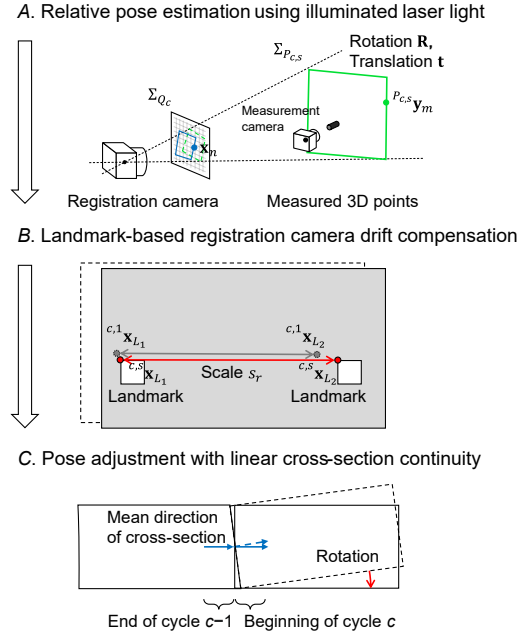


Fig. 2. Overview of the proposed pose adjustment

### A. Pose estimation based on the cross-section shape illuminated by an omnidirectional laser

A schematic of the relative pose estimation using the omnidirectional laser light is shown in Fig. 3. To perform 3D measurements of a long tunnel section without using environmental textures, the method by Igaue et al. [15] can be used, which divides the tunnel section into  $C$  measurement cycles for measurement. The measurement system consists of the following two cameras:

Measurement camera:

This camera performs 3D measurements based on line-structured light method. It is mounted on a UAV aimed at cross-section measurements.

Registration camera:

This camera captures the laser light illuminated from the UAV for cross-section measurements. 2D–3D registrations are conducted on a image plane of this camera for the relative pose estimations.

Here, 2D–3D registration represents the method to estimate relative poses between the two cameras by using 3D point clouds obtained from the measurement camera and 2D ray vectors obtained from the registration camera.

A long section of a tunnel are measured using the two cameras as the following procedures:

- 1) The measurement camera is moved to measure the 3D point clouds of the tunnel cross-sections based on the line-structured light method. Subsequently, the cross-section point cloud  $\mathcal{Y}^{c,s}$  ( $c = 1, 2, \dots, C, s = 1, 2, \dots, S_c$ ) is obtained, where  $c$  denotes the measurement cycle and  $s$  denotes the cross-section. The coordinate system of the measured cross-section is integrated based on the relative pose from the registration camera.

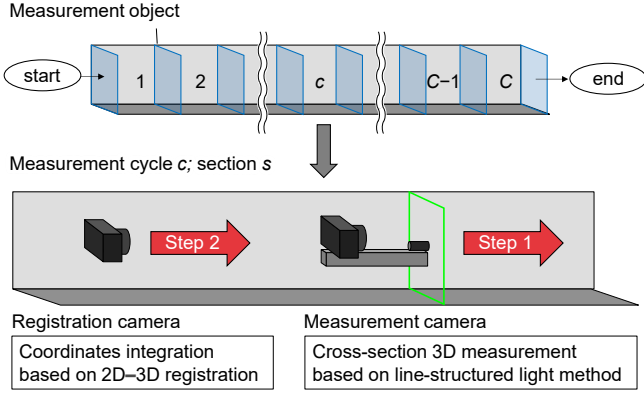


Fig. 3. Overview of the pose estimation method with 2D-3D registration of the omnidirectional laser light.

- 2) After measuring cycle  $c$  over a certain distance, the hovering position of the registration camera is updated to the hovering position in cycle  $c + 1$ .

The poses of all measured 3D cross-section point clouds are calculated using the image of the laser light acquired from the registration camera.

The following calculation is a method to estimate the pose of the measured cross-section in the registration camera coordinate system of cycle  $c$  ( $\Sigma_{Q_c}$ ). First, a 3D point cloud of the tunnel cross-section  ${}^{P_{c,s}}\mathcal{Y}$  ( ${}^{P_{c,s}}\mathbf{y}_m \in {}^{P_{c,s}}\mathcal{Y}$  ( $m = 1, 2, \dots, M$ )) is measured based on the line-structured light method. The relative pose of the registration and measurement cameras in  $\Sigma_{Q_c}$  is denoted by  ${}^{Q_c}\mathbf{T}_{P_{c,s}}$ . From this relative pose, it is possible to integrate all cross-section point clouds into the coordinate system of the first cycle using the following equation:

$$\begin{bmatrix} {}^{Q_1}\mathbf{y}_m \\ 1 \end{bmatrix} = {}^{Q_1}\mathbf{T}_{Q_2} \dots {}^{Q_{c-1}}\mathbf{T}_{Q_c} {}^{Q_c}\mathbf{T}_{P_{c,s}} \begin{bmatrix} {}^{P_{c,s}}\mathbf{y}_m \\ 1 \end{bmatrix}, \quad (1)$$

where  ${}^B\mathbf{T}_A \in \mathbb{R}^{4 \times 4}$  is a transformation matrix from  $\Sigma_A$  coordinate to  $\Sigma_B$  coordinate and  ${}^A\mathbf{y} \in \mathbb{R}^{3 \times 1}$  is a 3D point in  $\Sigma_A$  coordinate.

$${}^B\mathbf{T}_A = \begin{bmatrix} {}^B\mathbf{R}_A & {}^B\mathbf{t}_A \\ \mathbf{0}^\top & 1 \end{bmatrix}, \quad (2)$$

where  ${}^B\mathbf{R}_A \in \mathbb{R}^{3 \times 3}$  is a rotation matrix, and  ${}^B\mathbf{t}_A \in \mathbb{R}^{3 \times 1}$  is a translation vector.

${}^{Q_{c-1}}\mathbf{T}_{Q_c}$ , which indicates the pose of each cycle, is obtained using the estimated pose by 2D-3D registration. In the proposed method, when the measurement camera moves, the registration camera is fixed. Therefore, the cross-sections of cycle  $c$ ; section 1, and cycle  $c-1$ ; section  $S_{c-1}$  are in the same absolute poses. Therefore,  ${}^{Q_{c-1}}\mathbf{T}_{Q_c}$  is calculated using  ${}^{Q_{c-1}}\mathbf{T}_{P_{c-1,S_c}}$  and  ${}^{Q_c}\mathbf{T}_{P_{c,1}}$  as described by the following equation:

$${}^{Q_{c-1}}\mathbf{T}_{Q_c} = {}^{Q_{c-1}}\mathbf{T}_{P_{c-1,S_c}} {}^{P_{c-1,S_c}}\mathbf{T}_{Q_c}. \quad (3)$$

If  ${}^{Q_c}\mathbf{T}_{P_{c,s}}$  ( $c = 1, 2, \dots, C, s = 1, 2, \dots, S_c$ ) are known, all cross-sections can be integrated into  $\Sigma_{Q_1}$  using (1).

When the measurement camera performs the 3D measurement, the 3D point cloud is visible to the registration camera. The registration camera can, therefore, acquire a 2D point cloud of the tunnel cross-section  ${}^{Q_c}\mathcal{X}$  simultaneously as the 3D measurement of the cross-section. Then, using  ${}^{Q_c}\mathcal{X}$  and  ${}^{P_{c,s}}\mathcal{Y}$ , the 2D-3D registration is performed to estimate the pose of the measured cross-section point cloud. In this registration process, rotation matrix and translation vector optimizations are conducted as described with the following equation:

$$\arg \min_{{}^{Q_c}\mathbf{T}_{P_{c,s}}} -\mathcal{L}({}^{Q_c}\mathcal{X} | {}^{P_{c,s}}\mathcal{Y}, {}^{Q_c}\mathbf{T}_{P_{c,s}}). \quad (4)$$

Note that, this pose estimation is performed using a laser light projected on the cross-section. Therefore, this estimation is applicable even when there is no texture in the environment.

### B. Drift error reduction of cross-sectional point clouds using landmarks

The pose estimation method described in II-A assumes that the registration camera is stationary in the environment while the measurement camera is moving. However, a UAV cannot stop completely while hovering in the air. Consequently, drift errors occur in pose estimation because the registration coordinate system is not consistent through one measurement cycle. To reduce this drift error, the estimated translation vector of registration camera is compensated by the following method.

In tunnels, although objects such as construction machinery exist at certain intervals, they are not present at all points. Therefore, the proposed method uses the characteristic patterns of construction equipment as landmarks, that are always visible from the registration camera but not from the measurement camera. The registration camera keeps hovering near the landmarks to prevent them from being displaced on the image plane, thereby compensating for the drift. Note that the 3D coordinates of construction machinery left in a tunnel under construction are unknown in general cases. Therefore, we propose a method that can reduce drift using landmarks without 3D position informations. In this method, if there are no construction machinery near the registration camera, some characteristic features must be placed in the field of view of the camera.

The proposed method assumes that the registration camera keeps hovering at the points where two landmarks are visible. In this case, two feature points  ${}^{c,s}\mathbf{x}_{L_1}$  and  ${}^{c,s}\mathbf{x}_{L_2}$  are calculated as ray vectors from the registration camera of cycle  $c$ ; section  $s$ . At all measurement points in cycle  $c$ , the ray vectors at these two points are made to coincide with the ray vectors at cycle  $c$ ; section 1, on the image plane. Therefore, the set of ray vectors of laser points  $\mathbf{x}_n \in {}^{Q_{c,s}}\mathcal{X}$  ( $n = 1, 2, \dots, N$ ) is compensated using compensation matrix  $\mathbf{A}_r \in \mathbb{R}^{3 \times 3}$  and vector  $\mathbf{t}_r \in \mathbb{R}^{3 \times 1}$  as follows:

$$\hat{\mathbf{x}}_n = \mathbf{A}_r(\mathbf{x}_n - \mathbf{t}_r), \quad (5)$$

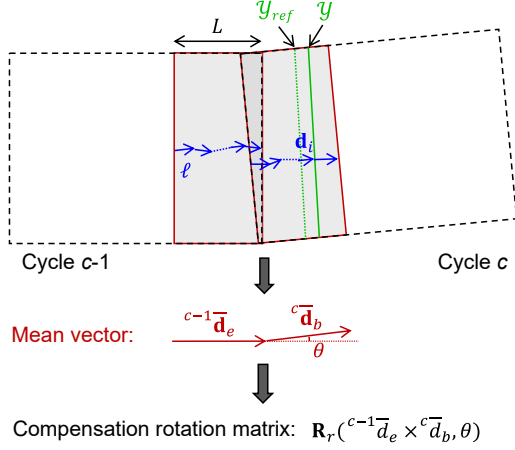


Fig. 4. Error reduction based on cross-section continuity.

where  $\mathbf{A}_r$  is an affine matrix that scales the ray vector by  $1/s_r$ , and  $\mathbf{t}_r$  is the two-dimensional translation at landmark on the image plane ( $z = 1$ ). The scale  $s_r \in \mathbb{R}$  and 2D translation vector  $\mathbf{t}_r$  from cycle  $c$ ; section 1, are calculated using two landmarks, which are always visible from the registration camera, as follows:

$$s_r = \frac{\|{}^{c,s}\mathbf{x}_{L_1} - {}^{c,s}\mathbf{x}_{L_2}\|}{\|{}^{c,1}\mathbf{x}_{L_1} - {}^{c,1}\mathbf{x}_{L_2}\|}, \quad (6)$$

$$\mathbf{t}_r = {}^{c,s}\mathbf{x}_{L_1} - {}^{c,1}\mathbf{x}_{L_1}, \quad (7)$$

where  ${}^{c,s}\mathbf{x}_{L_1}$  and  ${}^{c,s}\mathbf{x}_{L_2}$  are the ray vector coordinates of landmarks in cycle  $c$ ; section  $s$  frames. This allows us to compensate for drift by acquiring ray vectors obtained from the virtual viewpoints to which the UAV must be fixed.

A relative pose estimation of the two UAVs is performed with the stabilized ray vectors  ${}^{Q_{c,s}}\hat{\mathcal{X}}$  and the measured cross-section points  ${}^{P_{c,s}}\mathcal{Y}$  based on the 2D-3D registration in II-A. As a result, the pose of the UAV without the translation vector drift can be estimated.

### C. Reduction of pose estimation errors between cycles based on cross-section linearity

In the 3D measurement, which is alternatively operated using two UAVs, the measurement is divided into multiple cycles. This division causes an error in the calculation of the rotation matrix at the joints between the measurement cycles. To reduce this error, the proposed method utilizes the fact that the areas around the measurement cycles are connected linearly following assumptions:

- 1) At a distance  $L$  from the boundary of the measurement cycles, the translation of the measurement camera is arbitrary, but the rotation of the camera is consistent.
- 2) At a distance  $L$  from the boundary of the measurement cycles, the shape of the measured cross-section does not change.

An overview of the rotation matrix adjustment for the rotation error reduction is shown in Fig. 4. To simplify the explanation, the adjustment between cycle  $c-1$  and cycle  $c$  are described here. Near the boundary of each measurement

cycle, the direction of cross-section  $\mathbf{d}$  is calculated when the measurement camera has traveled a distance  $\ell$  ( $< L$ ). The mean cross-section movement  $\bar{\mathbf{d}}$  is calculated after travelling distance  $L$ . Here, as the measured cross-sections are assumed to be linearly aligned during distance  $L$ , the translation vector of the measured cross-section  $\bar{\mathbf{d}}$  is consistent at the joint of cycles. This characteristic is utilized to reduce the rotation estimation error by adjusting the poses of the point cloud of each measurement cycle.

The direction of cross-section  $\mathbf{d}$  is estimated by 3D-3D registration [16] of the two cross-sections. In the registration, the translation vectors are optimized and applied to the reference cross-section  $\mathcal{Y}_{ref}$  in coordinate  $\Sigma_{Q_1}$  to minimize the gap between  $\mathcal{Y}$  and  $\mathcal{Y}_{ref}$ . The following equation is used to calculate the direction of travel of the tunnel cross-section:

$$\mathbf{d} = \arg \min_{\mathbf{t}} -\mathcal{L}(\mathcal{Y}|\mathcal{Y}_{ref}, \mathbf{R}, \mathbf{t}), \quad (8)$$

where  $\mathbf{R}$  and  $\mathbf{t}$  are the rotation matrix and the translation vector, respectively, applied to the reference section. These matrices are initialized as the estimated results in II-A. As a result,  ${}^{c-1}\bar{\mathbf{d}}_e$  and  ${}^c\bar{\mathbf{d}}_b$  are calculated as direction vectors at the end of cycle  $c-1$  and the beginning of cycle  $c$ , respectively. Here, the 3D-3D registration are also conducted when the registration UAV moves  $\ell$  toward the tunnel wall owing to drift, even if the measurement UAV is not actually moving. This direction vector does not correspond to the tunnel road direction, and reduces the accuracy of the mean direction vector. Therefore, outliers are removed from the calculated vectors using the k-nearest neighbor [17]. The mean direction vector  $\bar{\mathbf{d}}$  of the cross-section is then calculated.

The rotation is adjusted by minimizing the deviation between the two mean vectors calculated above. When the angle between the two mean vectors is  $\theta$ , the compensation rotation matrix is calculated as follows:

$${}^{Q_c}\hat{\mathbf{R}}_{Q_{c-1}} = {}^{Q_c}\mathbf{R}_{Q_{c-1}}\mathbf{R}_r({}^{c-1}\bar{\mathbf{d}}_e \times {}^c\bar{\mathbf{d}}_b, \theta), \quad (9)$$

where  $\mathbf{R}_r$  is Rodrigues' rotation formula, given  ${}^{c-1}\bar{\mathbf{d}}_e \times {}^c\bar{\mathbf{d}}_b$  as a rotation axis and  $\theta$  as a rotation angle. Subsequently, the rotation-compensated point cloud of cycle  $c$  is obtained as  ${}^{Q_c}\mathcal{Y} {}^{Q_c}\hat{\mathbf{R}}_{Q_{c-1}}$ .

Rotation compensation is performed at the origin of the registration camera coordinate in cycle  $c$ . The rotation at this origin causes a misalignment at the junction of the point cloud of cycle  $c-1$  and cycle  $c$ . To compensate for the misalignment, the 3D-3D registration is also performed for the final section of cycle  $c-1$  and the first plane of cycle  $c$ , and a compensated translation vector  ${}^c\hat{\mathbf{t}}_{c-1}$  is obtained.

Finally, the bent point cloud is corrected by applying the compensated rotation matrix and translation vector as the following equation.

$${}^{Q_c}\hat{\mathcal{Y}} = {}^{Q_{c-1}}\hat{\mathcal{Y}} {}^{Q_c}\hat{\mathbf{R}}_{Q_{c-1}} + {}^{Q_c}\hat{\mathbf{t}}_{Q_{c-1}}. \quad (10)$$

The proposed method performs the aforementioned procedure to reduce measurement errors in 3D tunnel measurements over long distances.

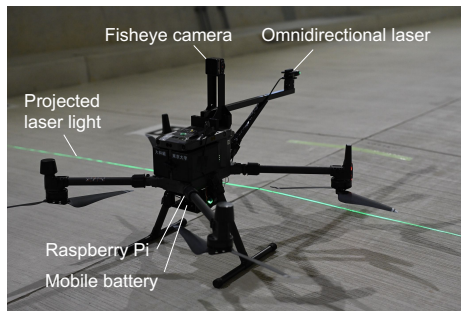


Fig. 5. Cross-section measurement system with UAV.



Fig. 6. Measurement conditions.

### III. EXPERIMENTS

#### A. Condition

The effectiveness of the proposed algorithm was verified using data from a 3D measurement experiment in a model tunnel. The UAV that was used as the measurement camera is shown in Fig. 5. The measurement camera was a Matrice 300 RTK equipped with action cameras (Kodak PIXPRO SP360 4K, 30 fps and  $2880 \times 2880$  pixels). A 30 mW laser that emits green light in a  $360^\circ$  direction was used as the omnidirectional laser. A Raspberry Pi 4 Model B was installed on the UAV to control the blinking of the omnidirectional laser. The DJI mini 2 with its built-in camera (30 fps,  $2720 \times 1530$  pixels) was used as the registration camera. Both UAVs were operated manually. The initial frames of the video measured by both cameras were visually matched after the images were acquired.

The measurement conditions are shown in Fig. 6. The model tunnel was 8.8 m wide and 6.4 m high. The measured area was approximately 30 m long. Experiments were conducted with the lighting in the tunnel turned on to obtain approximate measurements in a construction environment. We assumed that two landmarks exist in each 6 m section of the tunnel to estimate the translation vector and compensate for registration camera drift. Under this assumption, the length of one cycle in the measurement was set to 6 m. In this setup, the registration camera was moved closer to the measurement camera every time the measurement camera moved 6 m. AR markers placed in the environment were used as substitutes for landmarks with unknown coordinates. The AR markers were detected using the method described in [18] and [19].

TABLE I  
ANGLE BETWEEN  $\mathbf{d}$  AND MEAN VECTOR  $\bar{\mathbf{d}}$  IN ALL MEASUREMENT CYCLES

No stabilization	Proposed method
$0.17 \pm 0.10$ deg	$0.14 \pm 0.08$ deg

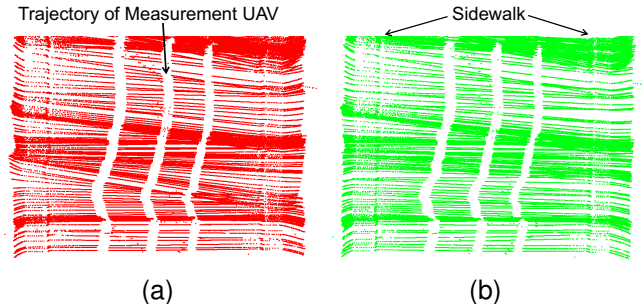


Fig. 7. Top view of the measured point clouds with and without drift compensation: (a) no stabilization and (b) proposed method.

The distance for estimating the direction of the measured cross-section was fixed to  $\ell = 100$  mm, and that of the area used for pose adjustment for each cycle was fixed to  $L = 1000$  mm. In the calculation of translation vectors by 3D–3D registration,  $M$  was set to 1000, and  $N$  was set to 100. In the outlier removal by k-nearest neighbor, the nearest points was set as  $k = 3$ , and the inlier was set as a direction vector with a mean among its neighbors within 0.3 rad.

#### B. Results and Discussion

1) *Drift error reduction of cross-sectional point clouds using landmarks:* Table I presents the standard deviation of the inlier of the k-nearest neighbors at the first and last 1 meter of every cycle. The measured tunnel has no curvature. Therefore, this value becomes smaller when lower drift errors occur approximately every 100 mm. The standard deviation of the calculated direction vectors was larger when no compensation was made, which is owing to the drift of the registration camera. In contrast, the proposed method could reduce the variation in the translation vectors by compensating the ray vectors from the registration camera.

The measurement point cloud of cycle 1 is shown in Fig. 7 as a drift-compensated point cloud. The pose of the measurement camera was estimated by 2D–3D registration using the omnidirectional laser. Therefore, the pose could be estimated even when the measurement camera was moved by the operator with rotation. When the measured cross-section point clouds were merged to coordinate  $\Sigma_{Q_1}$  of cycle 1, the contours of the cross-sections were wavy when the drift was not compensated. In contrast, with the compensation, the contour of the measured points approached a straight line, which is the actual shape of the tunnel. The shape of the measured point cloud also indicates that the stabilization of the ray vectors using landmarks in the proposed method is effective in reducing the drift.

2) *Reduction of pose estimation errors between cycles based on directional linearity:* The results of the 3D mea-

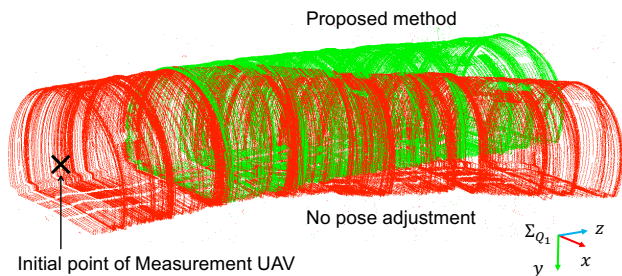


Fig. 8. Measured point cloud with and without pose adjustment. The length of the measured point cloud is approximately 30 m.

TABLE II

POSITION MEASUREMENT ERROR FOR THE CROSS-SECTION, MEAN, AND STANDARD DEVIATION OF THE ERROR FOR THE SEVEN SAMPLES AVERAGED OVER THE FOUR AR MARKERS CORRESPONDING TO THE CROSS-SECTION. EACH AXIS CORRESPONDS TO THAT OF FIG. 8.

	$x$ [mm]	$y$ [mm]	$z$ [mm]
No pose adjustment	$675 \pm 360$	$59 \pm 38$	$139 \pm 55$
Proposed method	$212 \pm 138$	$55 \pm 33$	$127 \pm 91$

surement for the entire measurements area is shown in Fig. 8. These point cloud was reconstructed from videos about five minutes and 38 seconds obtained from the measurement camera and registration camera. In the first cycle, the point cloud poses were consistent regardless of the rotation matrix compensation between cycles. However, once the distance between the measurement and registration cameras increased, the cross-section pose estimation error increased. Subsequently, all cross-section point clouds were merged as curved. In contrast, the proposed method resulted in a point cloud with no curvature that closely resembles the actual tunnel. The proposed method assumes that the joints of the cycles are on average straight. With this assumption, the proposed method successfully compensates for the curvature of the point cloud between cycles.

The position estimation errors for the AR markers placed at 6 m intervals are presented in Table II. The 3D position of each AR marker's origin was measured using the measurement camera image. Using this camera image, the 2D position of laser light in the pixel coordinate was calculated in addition to the AR marker positions. Thus, the 3D coordinates of the AR markers were calculated from the 2D laser points closest to the origins of the AR markers. Without compensation for the curvature at the joint area, the 3D measurement error was as large as 675 mm in the  $x$ -axis direction. The line-structured light-based 3D measurement device measures a large structure using a fisheye camera. Then, the largest calibration error was in the tunnel width direction because it had the largest dimension. Therefore, the largest errors occur along the  $x$ -axis. Despite the large pose estimation error in the  $x$ -axis direction, the error between cycles was greatly improved using the proposed method. This is because pose adjustment, which is based on the linear continuity of the measured cross-section at each cycle joint,

is suitable for 2D–3D registration-based 3D measurements of tunnels.

In addition, not only the coordinate estimation error of the measured cross-section in the  $x$ -axis, but also the measurement accuracy in the  $yz$ -axis direction improved. Therefore, the proposed method can provide accurate pose adjustment even when the coordinate estimation error is small, assuming that the joints of the cycle are nearly straight. With the proposed method, a distance of 30 m can be measured with an accuracy of 212 mm in the  $x$ -axis direction, where the error is the largest. Therefore, it is possible to locate deformations and defects in a tunnel with an accuracy of 212 mm over a distance of approximately 30 m from the starting point of measurement.

In addition, the proposed method assumes the presence of landmarks, such as construction equipment, at regular intervals but does not assume any texture in the tunnel. Therefore, it is possible to carry out 3D measurements with the same measurement accuracy even in tunnels without environmental textures.

#### IV. CONCLUSION

In this paper, we proposed a method to reduce the position estimation error of a measured cross-section from textureless 3D measurements based on the line-structured light method using two UAVs. The errors are caused by the drift of the UAVs and the pose discontinuity between measurement cycles. The proposed method solves the drift of the UAV by stabilizing the ray vector of the camera mounted on the UAV with respect to a landmark in the environment. The pose estimation error between measurement cycles is reduced by performing a pose adjustment, which takes advantage of the fact that the measured cross-sections are linearly continuous between measurement cycles. In the experiment, the ray vectors in drift compensations were calculated from the measured data in a model tunnel with pseudo landmarks. As a result, the drift of the measurement points could be surpassed. Furthermore, assuming that the cross-sections 1 m before and after the joint of each measurement cycle are linearly continuous, the directions of the measured cross-sections were compensated with an error of 212 mm in the axial direction, where the error was the largest, over a distance of 30 m.

In the future works, additional evaluations of the proposed method are conducted from the viewpoint of the analysis time. Moreover, detail analysis for the distance between the landmarks are also conducted because it affects the accuracy of 3D measurements. The future works also includes the next steps of the proposed method that is performing 3D measurements by setting up landmarks in a construction environment. In addition, the cross-section direction will be estimated nonlinearly at the joints of the measurement areas to reduce the error for tunnels with curvature.

#### ACKNOWLEDGMENT

This work was in part supported by JSPS KAKENHI Grant Number 22K18826 and a research fund by Kanto

REFERENCES

- [1] Y. Xue, X. Ma, D. Qiu, W. Yang, X. Li, F. Kong, B. Zhou, and C. Qu, "Analysis of the factors influencing the nonuniform deformation and a deformation prediction model of soft rock tunnels by data mining," *Tunnelling and Underground Space Technology*, vol. 109, p. 103769, 2021.
- [2] Z. Wang, X. Su, H. Lai, Y. Xie, Y. Qin, and T. Liu, "Conception and evaluation of a novel type of support in loess tunnels," *Journal of Performance of Constructed Facilities*, vol. 35, no. 1, p. 04020144, 2021.
- [3] J.-Y. Han, J. Guo, and Y.-S. Jiang, "Monitoring tunnel deformations by means of multi-epoch dispersed 3D LiDAR point clouds: An improved approach," *Tunnelling and Underground Space Technology*, vol. 38, pp. 385–389, 2013.
- [4] D.-J. Seo, J. C. Lee, Y.-D. Lee, Y.-H. Lee, and D.-Y. Mun, "Development of cross section management system in tunnel using terrestrial laser scanning technique," in *Proceedings of the XXIst ISPRS Congress*, vol. XXXVII, no. B5, 2008, pp. 573–581.
- [5] V. Gikas, "Three-dimensional laser scanning for geometry documentation and construction management of highway tunnels during excavation," *Sensors*, vol. 12, no. 8, pp. 11 249–11 270, 2012.
- [6] X. Xie and X. Lu, "Development of a 3D modeling algorithm for tunnel deformation monitoring based on terrestrial laser scanning," *Underground Space*, vol. 2, no. 1, pp. 16–29, 2017.
- [7] C. Wang, K. Li, G. Liang, H. Chen, S. Huang, and X. Wu, "A heterogeneous sensing system-based method for unmanned aerial vehicle indoor positioning," *Sensors*, vol. 17, no. 8, p. 1842, 2017.
- [8] A. Yamashita, K. Matsui, R. Kawanishi, T. Kaneko, T. Murakami, H. Omori, T. Nakamura, and H. Asama, "Self-localization and 3-d model construction of pipe by earthworm robot equipped with omnidirectional rangefinder," in *Proceedings of the 2011 IEEE International Conference on Robotics and Biomimetics*, 2011, pp. 1017–1023.
- [9] H. Higuchi, H. Fujii, A. Taniguchi, M. Watanabe, A. Yamashita, and H. Asama, "3D measurement of large structure by multiple cameras and a ring laser," *Journal of Robotics and Mechatronics*, vol. 31, no. 2, pp. 251–262, 2019.
- [10] M. Kawata, H. Higuchi, S. Pathak, A. Yamashita, and H. Asama, "Scale optimization of structure from motion for structured light-based all-round 3D measurement," in *Proceedings of the 2021 IEEE International Conference on Systems, Man, and Cybernetics*, 2021, pp. 442–449.
- [11] Y. Xue, S. Zhang, M. Zhou, and H. Zhu, "Novel SfM-DLT method for metro tunnel 3D reconstruction and visualization," *Underground Space*, vol. 6, no. 2, pp. 134–141, 2021.
- [12] C. Thomson, G. Apostolopoulos, D. Backes, and J. Boehm, "Mobile laser scanning for indoor modelling," *ISPRS Annals of Photogrammetry, Remote Sensing and Spatial Information Sciences*, vol. II-5/W5, 2013.
- [13] R. Kajaluoto, J. Hyypää, and A. Kukko, "Precise indoor localization for mobile laser scanner," *International Archives of the Photogrammetry, Remote Sensing and Spatial Information Sciences*, vol. XL-4/W5, pp. 1–6, 2015.
- [14] R. Kurazume, S. Nagata, and S. Hirose, "Cooperative positioning with multiple robots," in *Proceedings of the 1994 IEEE International Conference on Robotics and Automation*. IEEE, 1994, pp. 1250–1257.
- [15] T. Igaue, H. Higuchi, M. Ikura, K. Yoshida, S. Ito, N. Taniguchi, A. Yamashita, and H. Asama, "Ringu rēza shousha kou no 2D-3D macching ni motozuku hikarisesudanhō niyoru tonneru naibu no 3 jigen keisoku [line structured light-based tunnel 3D measurement with 2D-3D point cloud matching on projected light of ring laser]," *Journal of the Japan Society for Precision Engineering*, vol. 87, no. 12, pp. 987–994, 2021.
- [16] A. Myronenko and X. Song, "Point set registration: Coherent point drift," *IEEE Transactions on Pattern Analysis and Machine Intelligence*, vol. 32, no. 12, pp. 2262–2275, 2010.
- [17] S. Ramaswamy, R. Rastogi, and K. Shim, "Efficient algorithms for mining outliers from large data sets," in *Proceedings of the 2000 ACM SIGMOD International Conference on Management of Data*, 2000, pp. 427–438.
- [18] S. Garrido-Jurado, R. Muñoz-Salinas, F. J. Madrid-Cuevas, and R. Medina-Carnicer, "Generation of fiducial marker dictionaries using mixed integer linear programming," *Pattern Recognition*, vol. 51, pp. 481–491, 2016.
- [19] F. J. Romero-Ramirez, R. Muñoz-Salinas, and R. Medina-Carnicer, "Speeded up detection of squared fiducial markers," *Image and Vision Computing*, vol. 76, pp. 38–47, 2018.